NUCLEOLAR AND PERICHROMOSOMAL RNA SYNTHESIS DURING MEIOTIC PROPHASE IN THE MOUSE TESTIS

A. L. KIERSZENBAUM and LAURA L. TRES

From the Department of Anatomy and the Laboratories for Reproductive Biology, University of North Carolina, Chapel Hill, North Carolina 27514 and the Department of Anatomy, Duke University Medical Center, Durham, North Carolina 27710

ABSTRACT

The transcriptional activity during meiotic prophase in the mouse testis is studied with light microscopy and high-resolution autoradiographic techniques using [^{3}H]uridine as a labeled precursor. In the present study, two types of RNA synthesis are detected during meiotic prophase: an extranucleolar RNA synthesis of *perichromosomal* localization and a *nucleolar* RNA synthetic activity. In some of the autosomes and close to the basal knobs, the activity of the nucleolar organizers is evidenced by the incorporation of [^{3}H]-uridine into nucleolar masses from zygotene on and at earlier labeling times. The evolution of nucleoli and the formation of a nucleolus attached to the sex pair are described during the different meiotic stages. Perichromosomal labeling, from leptotene on, reaches a maximum during middle pachytene and falls progressively to a low level at longer incorporation times. Sertoli's cell, the most active RNA synthetic cell in the seminiferous epithelium, rises to a maximum of labeling and drops at earlier times compared with the meiotic prophase cells. The condensed sex chromosomes show some scattered silver grains especially at middle pachytene. The axial chromosome cores and synaptonemal complexes are devoid of silver grains during the meiotic prophase. The observations suggest that a control mechanism operates during meiotic prophase to regulate transcriptional activity in the sex chromosomes and to provide differential RNA synthesis in autosomal bivalents at various stages of prophase and within certain segments of the chromosomes.

INTRODUCTION

The evidence that RNA synthesis occurs during meiotic prophase is based largely on the autoradiographic localization of radioactive precursors incorporated by cells during the different stages of meiosis. Various species have been studied by several authors (1, 5, 6, 10, 11, 14, 35). These studies indicate that RNA is synthesized during one or more stages of meiotic prophase. Moreover, RNA synthesis in mouse (14, 15) and hamster (35) meiotic cells has been shown to occur exclusively on autosomes without indication of labeling of nucleoli or sex chromosomes. Nevertheless, meiotic cells are capable of nucleolar formation (10, 14, 22, 35) and, as far as we are aware, no incorporation of labeled RNA precursors has been found that could underlie nucleolar formation during meiotic prophase in the male. In the autosomes, the labeled RNA is concentrated more along the chromosomal margins than over the core of the chromosomes. In contrast to the

autosomes, the condensed sex chromosomes of the mouse (14) and hamster (35) appear inactive in RNA synthesis throughout the entire meiotic prophase. This differential behavior may be due to the fact that, in general, extended chromatin is more active in RNA synthesis than condensed chromatin, of which the sex chromosomes are examples. This explanation is consistent with the localization of the RNA-specific precursor [^{3}H]uridine along the length of all lampbrush bivalents in the diplotene stage of meiosis in amphibian oocytes (8), where the chromatin is clearly extended.

Recent studies have demonstrated extranucleolar RNA synthesis by the rapid incorporation of [^{3}H]uridine at the border of condensed chromatin in loci also occupied by perichromatin fibrils (7). The accumulation of inorganic cations in the periphery of the autosomal bivalents and in interchromatin areas during meiotic prophase in the mouse testis has also been described (34). In this last study it was suggested that the visualized inorganic cation accumulation could imply the presence of RNA polymerases, the activity of which is dependent on divalent cations; the patterns of intranuclear inorganic cation accumulation should indeed correlate with sites of RNA synthesis.

In the present study, the course of RNA synthesis has been followed during meiotic prophase in the mouse testis by autoradiographic localization of [^{3}H]uridine introduced into the testis at different intervals of time. In this paper, we present high-resolution autoradiographic evidence to support the existence of a genomic transcription at the nucleolar and perichromosomal loci in mouse meiotic cells. The evolution of nucleoli during meiotic prophase and the organization of the main nucleolus attached to the sex pair are also described.

MATERIALS AND METHODS

Adult male Swiss mice, ranging from 30 to 45 days old, were anesthetized with ether before the injection of [^{3}H]uridine ([5,6-^{3}H]uridine sp act 42.4 Ci/mmol, New England Nuclear, Boston, Mass.) used to label RNA. The radiochemical purity of [^{3}H]uridine determined by paper chromatography was initially greater than 99% and the percentages of radiochemical impurities were, for uracil, 0.2%, and deoxyuridine, 0.1% (lot no. 641-181). The experiment was repeated using different [^{3}H]uridine batches of sp act 40.4 Ci/mmol (lot no. 744-045) and 42.4 Ci/mmol (lot no. 642-172), respectively. The precursor was injected directly into both testes under the albuginea at a dose of 10 μCi per testis in a volume of 0.05 ml of sterile aqueous solution. We chose this route of injection on the basis of Monesi's results (14, 15) and because of the necessity to introduce the labeled compound directly into the incorporation site in an adequate and known testicular concentration in order to evaluate a possible rapid response in the very short postinjection intervals. The same route was used for prolonged labeling periods for suitable comparison. Testes were removed under anesthesia at the following postinjection intervals: 5, 15, 30, and 60 min; 3 and 24 h; 7, 8, 10, and 12 days. Aseptic suture was performed in the animals for postinjection intervals longer than 15 min. Control animals were injected with the solvent of the labeled precursor to check the morphology of germinal cells in the absence of [^{3}H]uridine.

Air-Dried Preparations

The tunica albuginea was removed and cells were dissociated from the seminiferous tubules by repeated aspiration and ejection using a syringe with isotonic saline solution. This procedure was performed on a watch glass kept on crushed ice. After a slight centrifugation to remove pieces of tubules and cell clumps, the suspension was centrifuged at 800 *g* for 10 min, and the resulting pellet was fixed with Carnoy's fixative (absolute alcohol 3 parts, glacial acetic acid 1 part). Centrifugations were carried out in an International Centrifuge PR-6 (International Equipment Co., Needham Heights, Mass.) with the temperature inside the centrifuge chamber set at 4°C. After resuspension in fresh fixative, preparations were made by rapidly drying a drop of suspension on a slide with the aid of a fan. The slides were dipped in Kodak Nuclear Track Emulsion NTB3 (Eastman Kodak Co., Rochester, N. Y.) and, after drying, put into black plastic side boxes with a desiccant (Drierite) to prevent latent image fading. The boxes were sealed with a black plastic tape and stored in a refrigerator at 4°C for exposure. The autoradiograms were developed with Kodak Developer D-19 for 30 s at 20°C after being exposed for 7–15 days. The slides were stained through the emulsion with methyl green-pyronine for 10 s for histochemical observations or with 1% Giemsa's stain in phosphate buffer (pH 7) for 2 min. Some preparations were stained with acetoorcein before coating with the emulsion.

High-Resolution Autoradiography

Small pieces of testes were fixed in 2.5% glutaraldehyde (biological grade) in 0.1 M phosphate buffer (pH 6.9) for 2 h at 4°C. They were then washed 3 times, 3 h each, in phosphate buffer (wash-

ing repeatedly the specimen facilitates the removal of unincorporated precursor), and postfixed in 2 % osmium tetroxide in 0.1 M phosphate buffer for 1 h at 4°C. The tissue was dehydrated in graded dilutions of ethanol and embedded in Maraglas. Sections of light gold interference color were obtained on a Porter-Blum ultramicrotome (Ivan Sorvall Inc., Newtown, Conn.) with glass knives. We used the flat substrate method for high-resolution autoradiography according to Salpeter and Bachmann (27). In this method, the sections were transferred to a Parlodion-coated (0.33% Parlodion in amyl acetate) half slide split lengthwise and with the edges smoothed. Care was exercised to avoid tearing the Parlodion film during this procedure. The excess of water was removed with a filter paper strip. Before coating with emulsion, the sections on the slides were stained with a few drops of an aqueous saturated uranyl acetate solution (for 15 min), followed by lead citrate (for 15 min). The stains were rinsed off by flushing with distilled water from a plastic washer bottle for a few seconds. A thin carbon layer (~50 Å) was vacuum evaporated over the stained sections. The slides were then coated with a diluted Ilford L4 emulsion by the dipping method. Ilford L4 emulsion was melted in a warm water bath at 45°C and 4 ml were diluted in 10 ml filtered distilled water. Dried slides were stored in sealed slide boxes as indicated for the air-dried preparations. After exposure for 25 days to 5 mo, the preparations were developed. The developers used were: Microdol-X (6.7 g in 100 ml of distilled water; developing time 4 min at 20°C); the gold latensification-Elon ascorbic acid procedure for punctuate grains according to Salpeter and Bachmann (27) modified by Wisse and Tates (36), and its modification for filamentous grains (28). Fixation was carried out with a fresh and filtered 20% solution of sodium thiosulfate in distilled water or with Kodak Rapid Fixer for 1 min. After fixing, the slides were rinsed in several changes of distilled water. Then, the specimen (a sandwich of Parlodion film, stained section, carbon layer, and developed emulsion, in that order) was stripped off the glass onto a water surface previously cleaned with optical lens tissue. The localization of the tissue sections was accomplished by the use of a dissecting microscope (10×) and copper grids (150-mesh) were placed over them. The specimen was picked up with a strip of Parafilm applied over it and kept in a Petri dish. The grids were carefully released from the remnant film by making small holes with the tip of a tweezer around the grid. In our experience, stripping the specimens was more difficult after development with Microdol-X than after the gold latensification procedure. The wire loop method (2) was also used with good results, although the above described flat substrate technique gave us more constant and reliable results. Most specimens were developed with the gold latensification-Elon ascorbic acid method. This technique shortens the exposure time by increasing the sensitivity of Ilford L4 about two- to threefold as a consequence of gold latensification before development (36). The background of the autoradiographs was very low for both the gold latensifications and Microdol-X developing procedures.

The grids were examined with a JEM 100B electron microscope operated at 80 kV with an objective aperture of 50 μm. The instrument was calibrated with a cross-lined, carbon grating replica having 1,350 lines/mm.

Thick Sections

A preliminary examination of autoradiographs of thick sections (0.5 μm thickness) was made in order to obtain an estimate of the duration of exposure for ultrathin sections, and also for selecting and locating the labeled regions; the embedded tissue was then oriented for ultrathin sectioning. Thick sections adjacent to the ultrathin ones were also obtained. The thick sections were deposited on glass slides and dipped in either Kodak NTB3 or Ilford L4 undiluted emulsions. After exposure for 10–20 days at 4°C, the preparations were developed in Kodak D-19 for 30 s and fixed in Kodak Rapid Fixer for 2 min. Once rinsed and air dried, the sections were stained through the emulsion with 1% toluidine blue in 1% sodium borate for 3 min at 40°C on a heated plate. The slides were washed in distilled water and mounted with Permount and regular cover slips. This technique gives satisfactory image of both tissue structure and silver grains with an increase in cytological details due to less superimposition of cells than is usually the case when thicker sections are used.

Timing of the Meiotic Prophase Cell Stages

In the testicular air-dried preparations, all stages from spermatogonia to mature spermatid could be recognized. The identification of individual cell stages was based on previous works (20, 31). For thick and ultrathin sections, the identification of the spermatogenic stages was also based on Oakberg's classification (20) slightly modified and on our own previous observations (34).

RESULTS

Autoradiography of Thick Sections

In preparations of testes fixed 5 min after intertesticular injection of [^{3}H]uridine, a few silver grains are predominantly located on the nucleoplasm of Sertoli's cells and on spermatogonial nuclei. No label was seen at this time either in the meiotic prophase spermatocytes or in immature

spermatids. After 15 min (Fig. 1) the nucleolus and nucleoplasm of Sertoli cells are seen covered with an increased number of silver grains. Spermatocytes start to show the presence of many grains distributed on the nucleoplasmic area. This pattern is well evident in middle pachytene spermatocytes (stage IV to VII); scattered grains are now visible in immature spermatid nuclei.

An increasing degree of labeling is seen after 30- and 60-min postinjection times. At 3 h, a comparison between stage X (Fig. 2) and stage V (Fig. 3) gives clear indication that at this time middle pachytene spermatocyte nuclei are heavily labeled in comparison to the late pachytene ones. In both spermatogenic stages the peripheral condensed sex chromosome pair is almost free of labeling. Sertoli cells are the most heavily labeled cells, and nucleoli are inferred by the presence of a well-delimited dark "hot spot" (Fig. 3). Due to this fact, Sertoli's cells were taken as control cells for the mean count estimates of silver grains in spermatocyte nuclei during the course of this study. Zygotene nuclei are also labeled and an apparently more concentrated distribution of grains is confined to the peripheral region of nuclei. This observation is not in complete agreement with Monesi's description that bivalent autosomes are labeled throughout the second half of meiotic prophase. Immature spermatid nuclei (step 5) show a diffuse labeling pattern (Fig. 3) in contrast to the lack of incorporation observed in late spermatid stages (i.e., step 10, Fig. 2).

A significant observation was noted between 7 and 12 days' exposure to the labeled compound. Nuclei of middle pachytene cells show a persistence of silver grains (Fig. 4), and these grains are progressively reduced in number toward day 12 (Fig. 5). The cytoplasm shows at this time the presence of scattered silver grains, some of which may be detected as early as 3 h after injection of [^{3}H]uridine. The sex pair does not show any relevant indication of labeling detected at the light microscopy autoradiographic level. In contrast to most of the spermatocyte stages, Sertoli's cell nuclei are totally free of silver grains after 7 days and a few of them are located near the

Abbreviations used on Figs. 1–7:
iS, immature spermatid *S, Sertoli's cell*
LP, late pachytene *Sg, spermatogonia*
MP, middle pachytene *XY, sex pair (also indicated by arrows)*
mS, mature spermatid *Z, zygotene*

FIGURE 1 Stage V. Labeling time: 15 min. Silver grains in nucleoli (crossed arrows) and nucleoplasm are visible in Sertoli's cells. Middle pachytene spermatocytes show labeling on the nucleoplasm whereas immature spermatids are almost free of silver grains. × 3,375.

FIGURE 2 Stage X. Labeling time: 3 h. Zygotene and late pachytene nuclei show silver grains contrasting with the absence of labeling in mature spermatids. Crossed arrow, nucleolus associated with the sex pair. × 3,375.

FIGURE 3 Stage V. Labeling time: 3 h. Sertoli's cell and middle pachytene nuclei are heavily labeled. Scattered silver grains are seen in nuclei of immature spermatids and in all cytoplasmic structures. Nucleoli of Sertoli's cells are inferred by a circumscribed black spot inside the nucleus. × 3,375.

FIGURE 4 Stage V. Labeling time: 8 days. Sertoli's cell and immature spermatid are almost unlabeled. Middle pachytene nuclei show persistence of silver grains in perichromosomal loci. Spermatogonia nuclei show a few grains. × 3,530.

FIGURE 5 Stage V. Labeling time: 12 days. A few residual silver grains can be recognized in middle pachytene nuclei and cytoplasm. Crossed arrow, nucleolus attached to its nucleolar organizer region. × 3,530.

FIGURE 6 Air-dried preparations. Labeling time: 60 min. A middle pachytene nucleus shows the unlabeled sex pair and the distribution of silver grains along the autosomes. × 3,300.

FIGURE 7 Air-dried preparation. Labeling time: 3 h. Same distribution as in Fig. 6. The XY pair remains practically unlabeled. The distribution of silver grains is difficult to localize due to the heavy labeling. Crossed arrow, nucleolar mass attached to the XY pair. × 3,600.

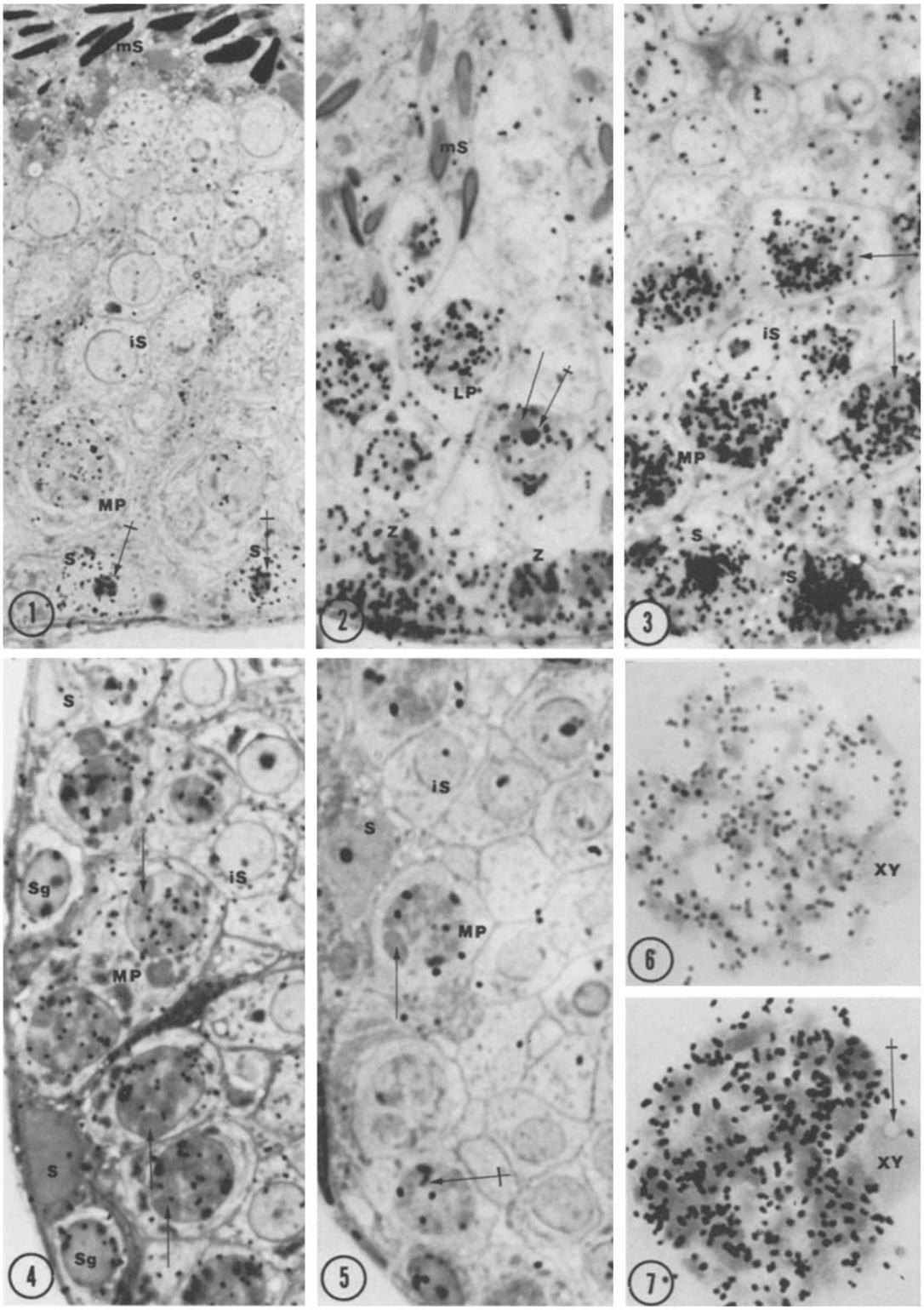
mS
iS
MP
S
S
1
mS
LP
Z
Z
2
iS
MP
S
S
3
S
Sg
iS
MP
S
Sg
4
iS
S
MP
5
XY
6
XY
7

nuclear envelope of immature spermatids. Some spermatogonial cells still remain labeled. The decrease of labeling is significant at 12 days (Fig. 5). In this connection we may add that the absence of silver grains in Sertoli's cells during this period may rule out the existence of a persistent radioactive pool at the site of injection capable of maintaining the labeling of spermatocytes.

Autoradiography of Air-Dried Preparations

We used this approach for purposes of comparison with Monesi's data of RNA synthetic activities in the mouse testis, and for the evaluation of our own results using high-resolution autoradiographic techniques. One advantage of the air-dried preparations is that all cell stages are present in a single preparation. Also, the localization of the radioactive sources corresponding to reduced silver grains can be accomplished in the entire air-dried cell, and quantitation, such as the estimation of mean grain count per nucleus, can be done with proper regard for lightly and heavily labeled cells. The use of low temperature (4°C) during the resuspension and centrifugation procedures provides to some extent for slowing down and eventual stopping of RNA synthesis during the technical manipulation; at the same time it seems to preserve the nucleolar components. This can be particularly well evaluated by staining air-dried preparations with methyl green-pyronine before coating with photographic emulsion. Total nuclear grain count estimates for Sertoli's cells, the different stages of meiotic prophase—especially zygotene, middle, and late pachytene—and immature spermatids are shown in Fig. 8. The graphic profile indicates a close relationship to the results obtained with thick sections. In middle pachytene nuclei at 60 min the silver grains can be detected along the margins of the autosomes (Fig. 6). This feature cannot be easily recognized at 3 h due to the heavily labeled nuclei (Fig. 7). In less extended cells where the cytoplasmic structure is visible, the finding of silver grains in middle and late pachytene and diplotene suggests the transport of nuclear synthesized RNA into the cytoplasm. Metaphase I meiotic cells show a few grains in the chromosome margins and in the cytoplasm. The condensed sex chromosomes are clearly and invariably unlabeled during the different stages of the meiotic cycle, at least at the light microscopy level from zygotene on, in contrast to the autosomes (Figs. 2, 3, 6, and 7).

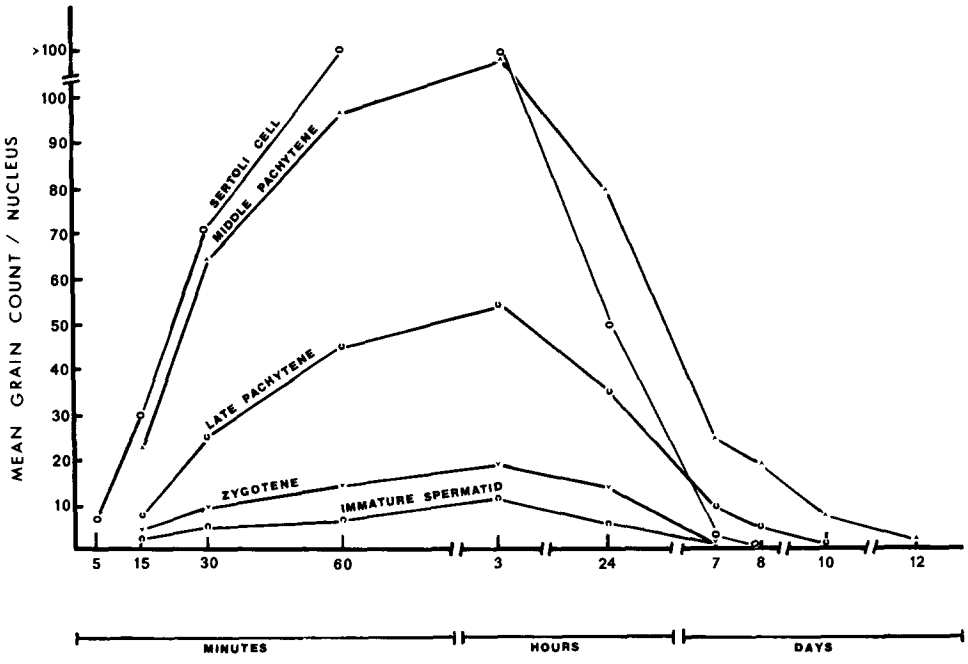

FIGURE 8 Patterns of RNA synthesis during meiotic prophase in the mouse. Nuclear grain count estimates from selected germinal cell stages compared with Sertoli's cell. The data were obtained by counting 60 cells per cell type in air-dried preparations and compared with counts obtained in photomicrographs. Leptotene, early pachytene, diplotene, and diakinesis stages are not indicated in this figure.

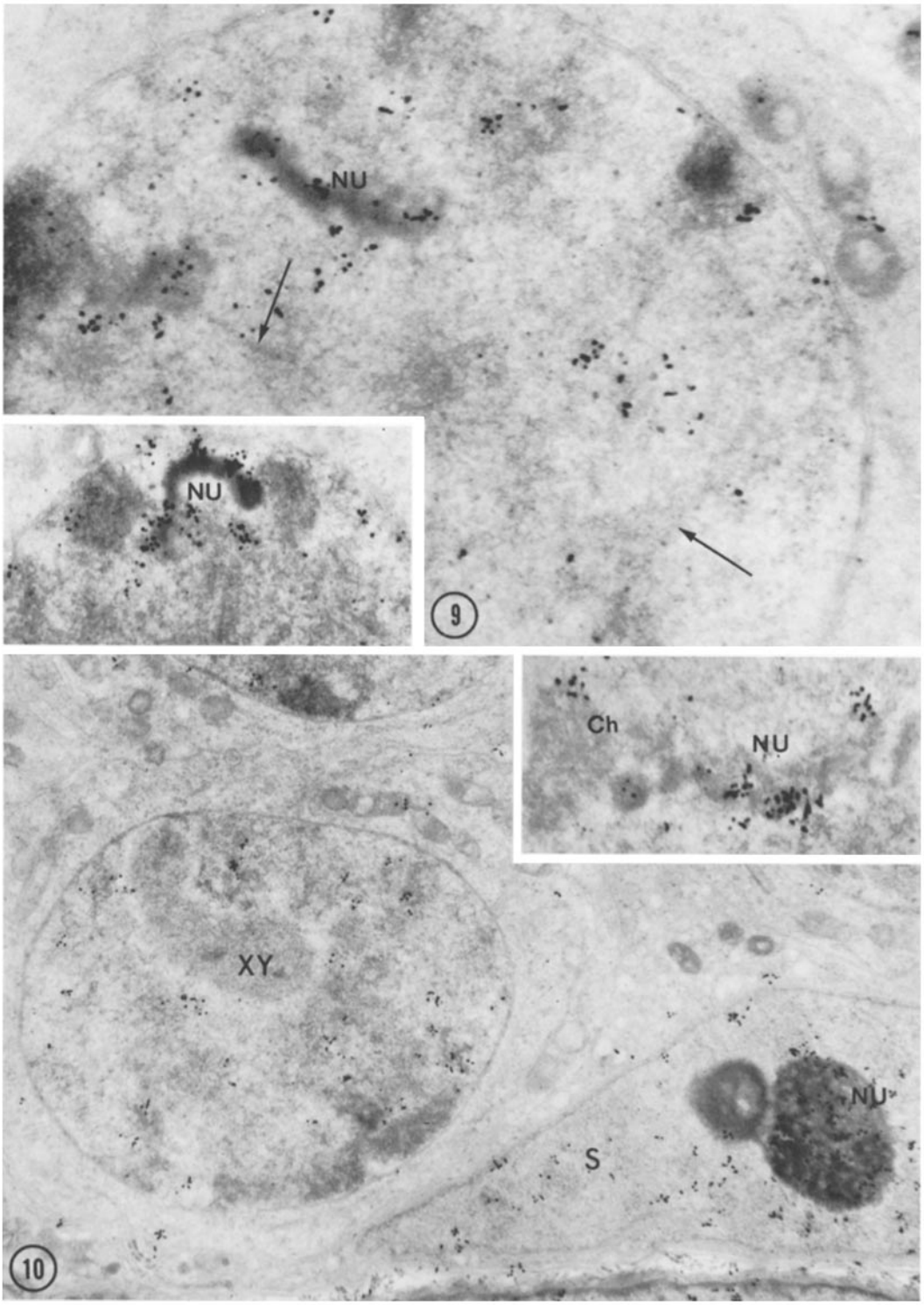

FIGURE 9 Zygotene spermatocyte. Labeling time: 3 h. Gold latensification Elon ascorbic acid (EAA) developing procedure. Silver grains are detectable in close proximity to the chromatin. A fibrillar nucleolus (*NU*) connected with condensed chromatin blocks (*inset*) are labeled. Arrows point out to unlabeled axial chromosome cores. × 22,500. *Inset*, × 16,000.

FIGURE 10 Early pachytene spermatocyte. Labeling time: 3 h. EAA. The unlabeled sex chromosomes (*XY*) are well distinguished. Scattered silver grains are seen in the expected perichromatin sites. The nucleolus (*NU*) and the nucleoplasm of a Sertoli's cell (*S*) are well labeled. The condensed chromatin body associated with the nucleolus remains unlabeled. × 9,600. *Inset*: Elongated and branched nucleolar mass (*NU*) with fibrillar and granular components. *Ch*, basal knob. × 20,000.

High-Resolution Autoradiography

The results obtained in thick sections and spread preparations, together with previous results obained by several authors in the mouse (14, 15) and hamster (35), confirm the assumption that autosomes, in contrast to the sex chromosomes, incorporate [^{3}H]uridine during the meiotic prophase. This incorporation is prominent during the middle pachytene stage. Although the presence of nucleolar structures associated with the autosomes and sex chromosomes has been described with conventional electron microscope techniques (30, 31, 34), the incorporation of RNA precursors could not be detected at the light microscopy autoradiographic level on those structures. Our results with the use of high-resolution autoradiographic techniques show that [^{3}H]uridine is incorporated into nucleoli during meiotic prophase in the mouse testis (also in the hamster, unpublished observation) and that it can be detected as early as 15 min after the intratesticular injection of the labeled compound. Therefore, two types of RNA synthesis are discernible and clearly detected during the meiotic prophase: and *extranucleolar* synthesis of perichromosomal localization and a *nucleolar* RNA synthetic activity.

In spermatocytes at pachytene stage, labeled nucleolar masses are attached to condensed chromatin blocks which, in turn, are connected to the nuclear envelope (Figs. 16 and 17). These blocks correspond to the paracentromeric heterochromatin of mouse telocentric chromosomes where satellite DNA is located (38). As described earlier by Woollam and Ford (37), a synaptonemal complex is interposed in the middle of these "basal knobs." As the synaptonemal complex is a structure associated with the pairing of homologous chromosomes (17), the "pairing" behavior of heterochromatin blocks is conspicuous (12).

At 3 h postlabeling, [^{3}H]uridine incorporated into *zygotene* spermatocytes (Fig. 9) is seen in the expected perichromosomal localization and particularly over the fibrillar nucleolar structure closely related to the condensed chromatin areas near the nuclear envelope. No silver grains are recognized along the axial chromosome cores of autosomes. *Early pachytene* cells show a disperse localization of silver grains always in close relationship to the autosomal chromatin. The sex chromosome pair is not labeled and a nucleolar band-shaped structure (Fig. 10) shows aggregates of silver grains over the apparent fibrillar component whereas the granular one, starting to be visible at this stage, is practically devoid of silver grains. This stands in contrast to the relatively high amount of silver grains observed on Sertoli's cell nucleoli in the same seminiferous tubule area. In *middle pachytene* cells at the same period of time, the heavy labeling pattern, which indicates a large amount of newly synthesized RNA, is evidenced by the gold latensification-Elon ascorbic acid procedure (Fig. 11), by its modification for filamentous grains (inset, Fig. 11), and by Microdol-X (Fig. 12). From the analysis of these autoradiograms it can be stated that nucleolar RNA synthesis is equally demonstrated with the three developing techniques; that extranucleolar RNA synthesis in its perichromosomal localization (Fig. 12) is higher at this stage when compared with zygotene and early pachytene stages; that the sex chromosomes, despite showing a few silver grains, do not show a particular or remarkable silver grain distribution on their structure; that the passage of nuclear synthesized RNA is reflected by the presence of silver grains on the cytoplasm (Fig. 12); and that a small labeled nucleolar mass is seen attached to the nucleoplasmic side of the distinctive condensed sex chromosomes (inset, Fig. 11).

FIGURE 11 Middle pachytene spermatocyte. Labeling time: 3 h. EAA. A large number of silver grains are seen scattered throughout the nuclei with a more concentrated distribution at the nucleolus (*NU*). Small masses of nucleolar elements (arrows) and a fibrillo-granular body are closely located to the unlabeled XY chromosomes. × 20,000. *Inset*: A modification of the developing procedure for filamentous silver particles (27) shows a very heavy labeling pattern in the nucleolus (*NU*) and in a small nucleolar portion attached to the XY chromosomes. × 9,600.

FIGURE 12 Middle pachytene spermatocytes. Labeling time: 3 h. Developing procedure Microdol-X. An arrow points to a synaptonemal complex without labeling. At this level, the chromatin of the paired chromosomes shows the peripheral localization of silver grains. The sex chromosomes (*XY*) are unlabeled. A nucleolus (*NU*) associated with a condensed chromatin mass is seen labeled. × 5,750.

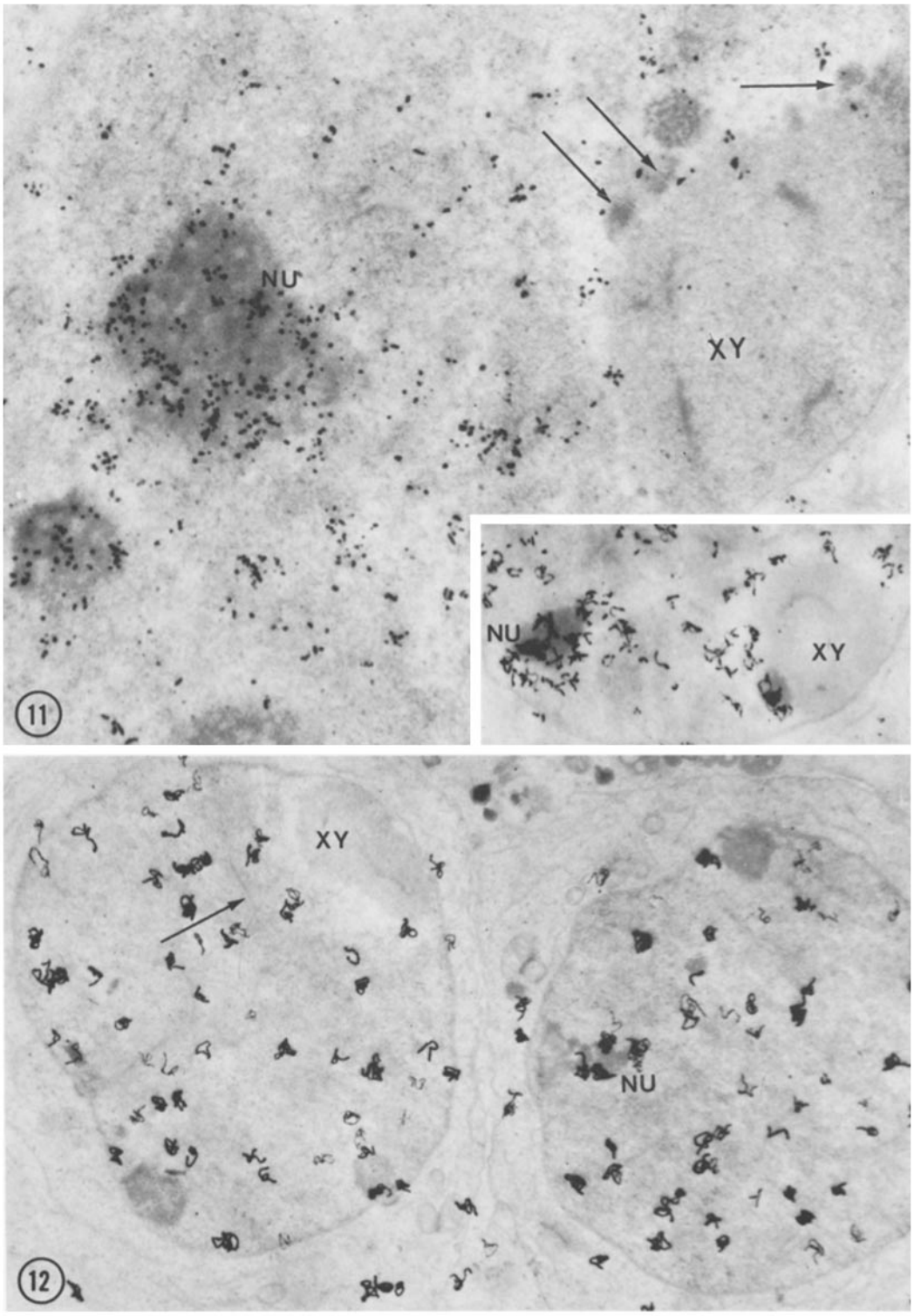
NU
XY
11
NU
XY
XY
NU
12

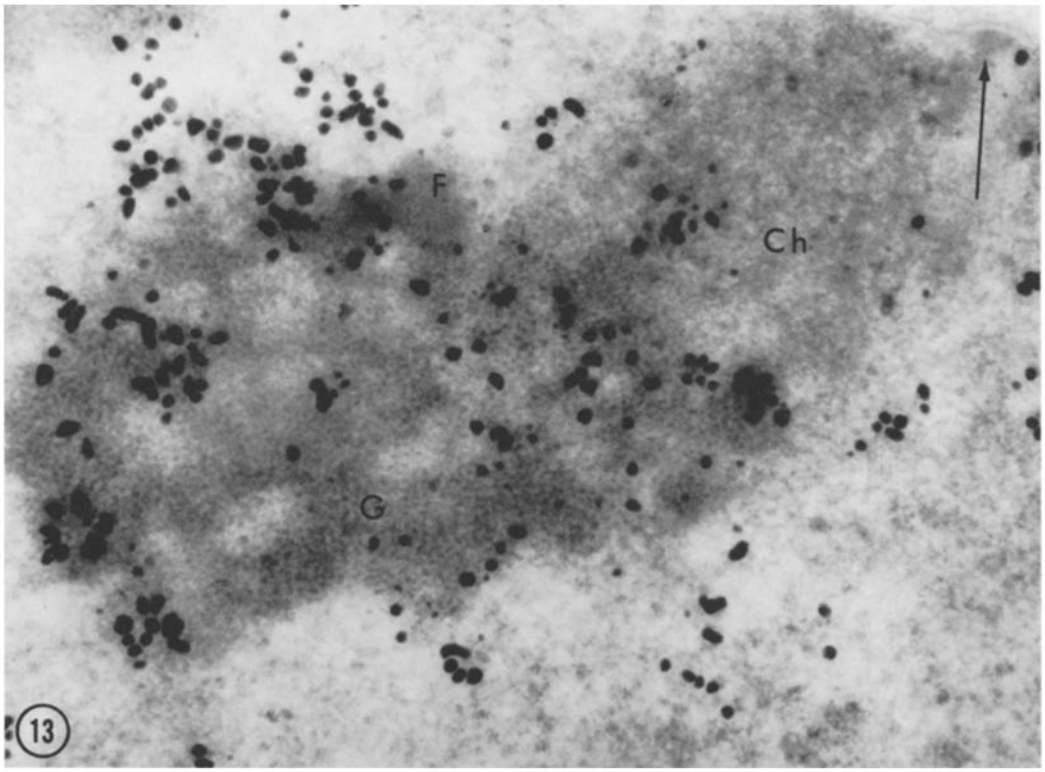
F
Ch
G
13

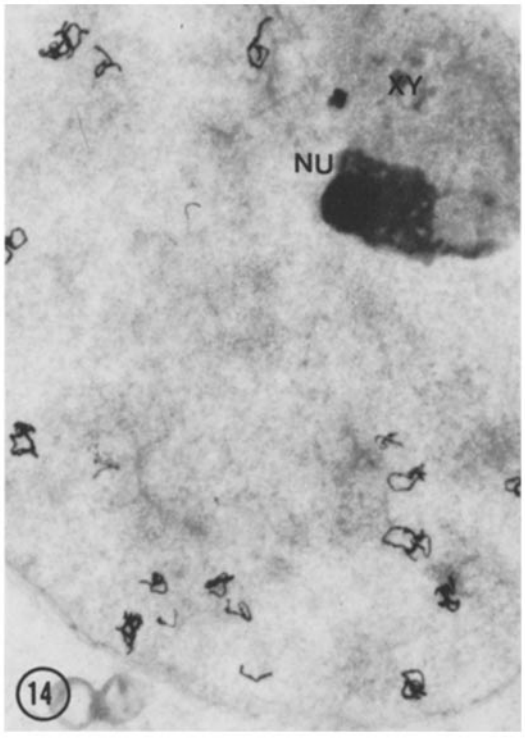
XY
NU
14

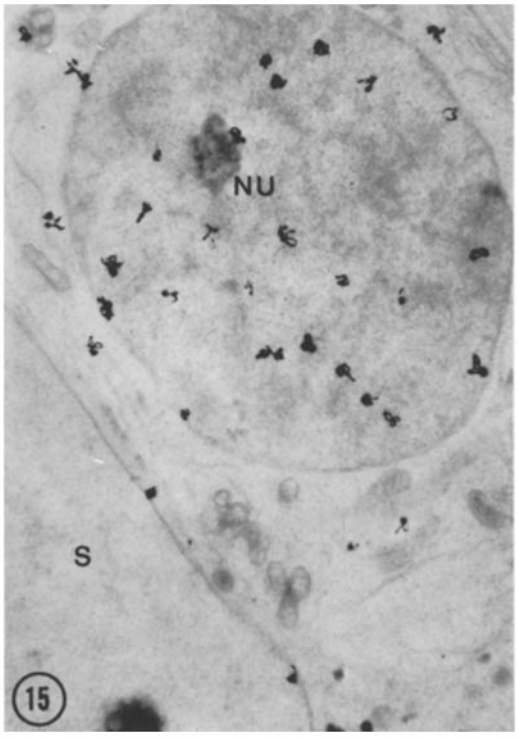
NU
S
15

The fibrillar and granular components of the nucleolar structure attached to the basal knob are shown in Fig. 13. Silver grains are localized at the periphery of the fibrillar component and, to a lesser degree, as well on the granular component. The contacting and well-delimited, dense chromatin area of the basal knob is not labeled, whereas the adjacent nucleoplasm contains scattered radioactivity. *Late pachytene* spermatocytes show a decrease of labeling at the chromosomal borders, but no grains are detected either on the sex pair or in its fully developed nucleolus (Fig. 14). Diplotene and diakinesis stages (not shown here) showed little RNA synthesis.

After 8 days of labeling, a pachytene spermatocyte, probably in zygotene stage at the time of labeling, still shows silver grains on the nucleus (Fig. 15). A portion of a nucleolus is free of label, as well as the nucleus of a Sertoli's cell. It is worthwhile to indicate that during the formation and development of the synaptonemal complex no detectable labeling with [^{3}H]uridine has been associated with this structure.

The incorporation of [^{3}H]uridine into nucleolar RNA during the middle pachytene stage and the organization of the nucleolus attached to the sex pair are shown through Figs. 16–20. A basal knob is seen attached to the nuclear envelope together with a portion of a synaptonemal complex (Figs. 16 and 17). In continuity with this condensed structure and separated by it from the nuclear envelope, a nucleolar mass, with characteristics already described in Fig. 13, is seen extending into the nucleoplasm. At the zygotene stage, the nucleolar mass is mostly fibrillar (Fig. 9) and the granular components start to be visible at early pachytene (Fig. 10, inset). The resolution obtained with the gold latensification procedure (Fig. 16) in comparison with Microdol-X (Fig. 17) seems to indicate the preferential localization of silver grains at the limit between the nucleoplasm and nucleolar components, predominantly in the fibrillar area. The remaining connection of a nucleolar mass directed toward the sex chromosomes is shown in Fig. 18. A nucleolar mass apparently detached from its basal knob connection, at least in the incidence of this section, seems to get closer to the sex chromosomes (Fig. 11), to make contact (Fig. 19), and to extend around them (Fig. 20). From this apparent sequence of events, it seems quite probable that the nucleolar masses originating at the paracentromeric nucleolar organizer regions, near the basal knobs, are concerned with the origin of the nucleolar material which will become associated with the nucleoplasmic part of the sex chromosomes.

DISCUSSION

The present autoradiographic observations in the mouse testis indicate that almost all RNA transcribed during meiotic prophase is localized in the perichromosomal region of bivalent autosomes. Additional nucleolar RNA synthesis in definable regions of some autosomes can also be detected. Furthermore, the rate of RNA synthesis in the sex chromosomes, as judged by [^{3}H]uridine incorporation, appears to be insignificant when compared with the rate in bivalent autosomes.

Earlier studies of RNA synthesis during meiosis in the mouse have indicated that autosomes do not participate in nucleolar formation (22). The heteropycnotic sex chromosomes, associated with the nucleolus, were thought to be involved in the formation of a nucleolar structure through a presumed activity of nucleolar organizers at this level (26). Autoradiographic studies with [^{3}H]uridine in mouse (14, 15) and hamster (35) testes have

FIGURE 13 Middle pachytene nucleus. Labeling time: 3 h. EAA. A nucleolus formed by fibrillar (*F*) and granular (*G*) components is seen labeled and attached to a basal knob (*Ch*). The arrow indicates a probable lateral element of a synaptonemal complex ending against the nuclear envelope. × 59,000.

FIGURE 14 Late pachytene spermatocyte. Labeling time: 3 h. Developing procedure: Microdol-X. The XY pair and the associated nucleolus (*NU*) are unlabeled. Some silver grains are seen in their perichromosomal localization. × 11,900.

FIGURE 15 Pachytene spermatocyte. Labeling time: 8 days. Developing procedure: Microdol-X. Silver grains are seen in the nucleus and cytoplasm. The nucleolus (*NU*) is unlabeled. A Sertoli's cell (*S*) is free of silver grains inside the nucleus. × 7,200.

demonstrated high autosomal RNA synthesis during middle and late pachytene stages, respectively, without evidence of incorporation of RNA precursors by the sex chromosomes. Moreover, no RNA synthetic activity has been revealed in the well-identified large nucleoli during the entire meiotic prophase in those species, suggesting that this is, at least in the hamster, one of the few cases of nucleolar metabolic inactivity (35).

Biochemical data on microsporocytes cultured in vitro (32) has indicated that the RNA formed at earlier meiotic stages is predominantly of the nonribosomal type, and it was concluded that ribosomal RNA is apparently absent during meiotic prophase. More recently, little nascent ribosomal RNA was inferred in lily microsporocytes after leptotene (23). Similar results were obtained from sedimentation analyses of isolated pachytene nuclei in the hamster (18).

It is conceivable, on the basis of our high-resolution autoradiographic observations, that, during the meiotic prophase, there is a mechanism regulating gene activity which keeps transcriptional activity low in the sex chromosomes and permits differential RNA synthesis in autosomes at certain defined stages of the prophase and in certain segments of bivalents. This assumption, with the premise that cells contain identical genomes, is based on (*a*) the scarce labeling of sex chromosomes during the 12 days that are considered the period necessary to complete the whole meiotic prophase (21); (*b*) the quantitative variations of autosomal RNA synthesis during the different stages; and (*c*) the localized nucleolar RNA activity at some of the basal knobs.

It is well known that condensed mitotic chromosomes fail to support RNA synthesis (33, 25). In meiotic chromosomes, RNA synthesis slows down as bivalent contraction progresses (i.e., in diplotene, diakinesis, and metaphase I). Certainly, good evidence of this correlation is given by the relative inactivity of the condensed sex chromosomes during the meiotic prophase.

During middle pachytene, the rate of perichromosomal incorporation increases to a maximum when compared with leptotene, zygotene, early and late pachytene, diplotene, and diakinesis. It has been proposed on the basis of autoradiographic evidence that the newly synthesized heterogeneous nuclear RNA (3, 4) is located adjacent to the chromatin (13, 7) in the form of perichromatin fibrils (7). If this is the case for the perichromosomal labeling during meiotic prophase, as it seems to be in hamster pachytene nuclei (18), it can be concluded that the rate of heterogeneous nuclear RNA synthesis rises to higher levels during middle pachytene. The localization of high RNA polymerase activity at this stage (16), the perichromosomal accumulation of pyroantimonate deposits in which the microprobe analysis detected several cations presumably related in part to RNA polymerase activity (34) during middle pachytene, and the fuzzy appearance of pachytene autosomes due to lateral projections of chromatin fibers, suggest that the DNA template becomes activated for transcriptional work along the bivalent margins.

The persistence of perichromosomal labeling at 7–8 days after [^{3}H]uridine injection in pachytene cells, when almost no label is found in the very active Sertoli's cell, suggests that a significant amount of the heterogeneous rapidly turning-

FIGURE 16 Labeled nucleolus (*NU*) is seen in direct continuity with a basal knob (*Ch*). A synaptonemal complex is ending against the nuclear envelope. Labeling time: 3 h. EAA. × 28,000.

FIGURE 17 Same as Fig. 16. Note the expansion of the lateral element of the synaptonemal complex. Developing procedure: Microdol-X. × 35,700.

FIGURE 18 A nucleolus (*NU*) which still maintains some connection with the basal knob region is also seen closely related to the XY pair. An arrow points to a small nucleolar mass probably originating in an extension of this nucleolus. Labeling time: 3 h. EAA. × 28,800.

FIGURE 19 A nucleolar mass (*NU*) is seen at the nucleoplasmic side of the XY pair. A few grains are seen scattered throughout the condensed sex chromosomes. Labeling time: 3 h. EAA. × 32,000.

FIGURE 20 A predominantly granular nucleolar mass (*NU*) surrounds the XY pair. Silver grains are diffusely arranged on the XY pair starting from the nucleolar mass border. Labeling time: 3 h. EAA. × 33,000.

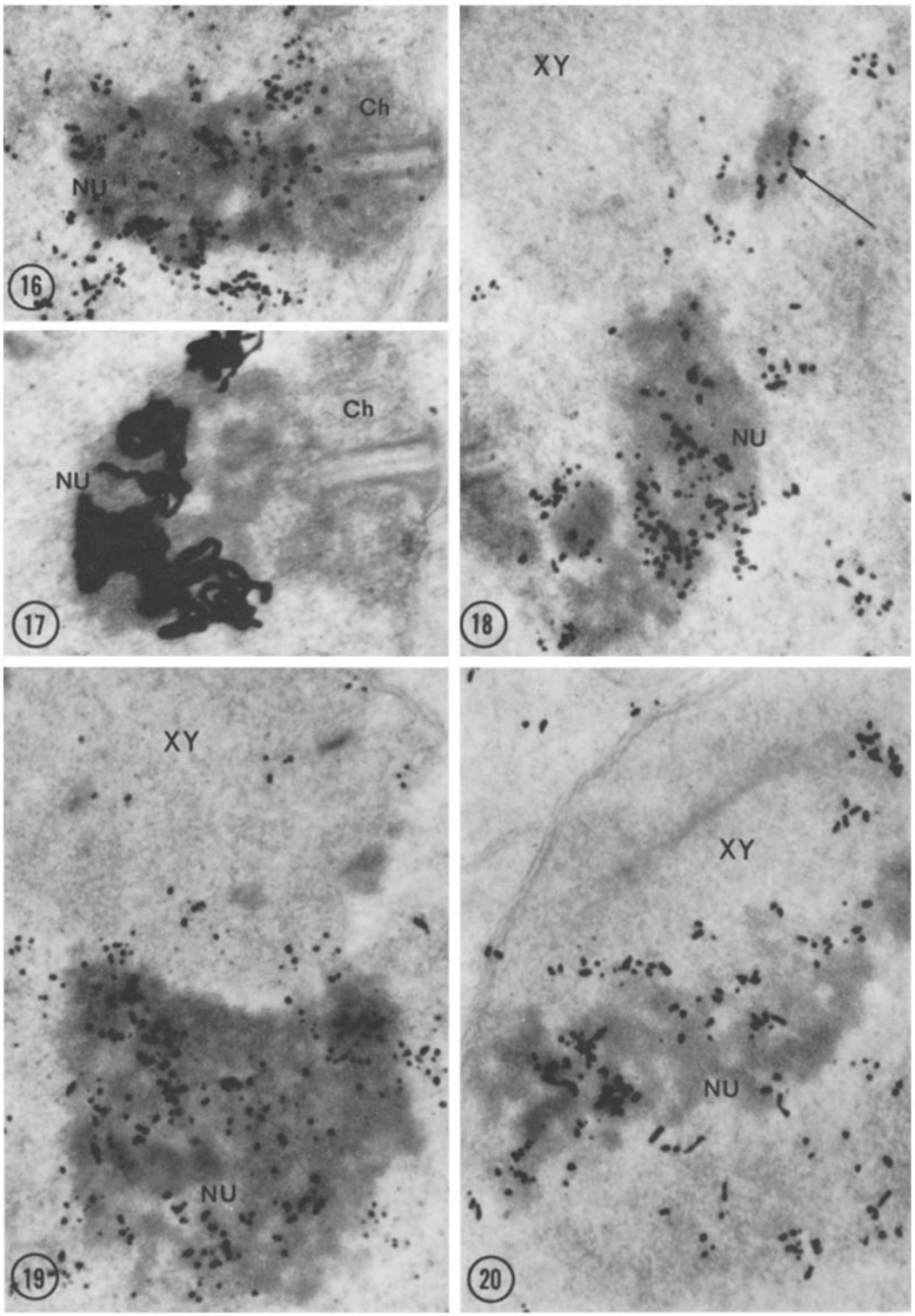
Ch
NU
16
Ch
NU
17
XY
NU
18
XY
NU
19
XY
NU
20

over nuclear RNA (4) is metabolized in the nucleoplasm and that the remaining silver grains probably correspond to disintegrating products.

One of the most interesting findings of this investigation is the presence of labeled nucleolar masses adjacent to basal knobs. This suggests that at this level some autosomes contain the nucleolar organizer region and that preribosomal RNA cistrons are activated from zygotene on. Although perichromosomal RNA synthesis was seen during leptotene, no conclusive nucleolar synthetic activity was detected at this stage. Nucleolar formation starts by the appearance of a fibrous labeled component at zygotene, followed by the granular component appearing at early pachytene. During middle pachytene, nucleolar development continues with increase of both fibrillar and granular components. Such a sequence argues against the possibility that nucleoli may arise from material retained from premeiotic stages.

Since nucleolar organizers are close to the paracentromeric condensed chromatin of several bivalent autosomes, the behavior of these regions in the X and Y chromosomes must be taken into account. The available data at the light microscopy level indicate that all telocentric mouse chromosomes, including the Y chromosome (24, 29), possess paracentromeric heterochromatin (12). At the high-resolution level, a condensed chromatin mass has been described at the free end of the X chromosome at zygotene (30). A similar condensed region, although less delimited, is also described in relation to the short core of the Y chromosome. These condensations are no longer visible in subsequent stages. Some observations should be pointed out in this respect. (*a*) The condensed chromatin mass attached to the nuclear envelope and seen at the free end of the X chromosome during zygotene does not organize a nucleolar structure, nor is it labeled in the same way as is the nucleolar organizer in an autosomal bivalent. (*b*) Labeled fibrillar nucleolar structures associated with autosomal condensed chromatin blocks during zygotene contrast with the lack of similar activities in the XY pair (as seen in the present study). (*c*) During middle pachytene, dense granules start accumulating on the nucleoplasm side of the sex pair. At late pachytene the nucleolus associated with the XY pair is fully developed.

If we accept that nucleolar formation during meiotic prophase starts first with appearance of a fibrillar component which serves as precursor for the granular member (9, 19), it follows that the appearance of the granular component during middle pachytene together with coalesced labeled nucleolar masses originating in autosomal nucleolar organizer regions, strongly suggest that there is little nucleolar organizer activity in the sex chromosomes themselves. The presence of silver grains during pachytene in the sex chromosomes is almost likely related to perichromosomal RNA synthetic activity in some decondensed areas, or to invaginations of nucleolar elements.

The authors are grateful to Dr. H. S. Bennett for facilities and Dr. M. J. Moses for his suggestions and criticisms of the manuscript.

This research was supported by a grant from The Rockefeller Foundation to the Laboratories for Reproductive Biology, University of North Carolina, Chapel Hill, N. C.

Received for publication 5 July 1973, and in revised form 7 September 1973.

Note added in proof: We have isolated meiotic chromosomes of the mouse testis and have displayed them in whole mount spreads, combined with high resolution electron microscopy autoradiography (manuscript in preparation). These studies using [^{3}H]uridine-labeled spermatocytes show, in some of the autosomal bivalents, a satisfactory preservation of nucleoli attached to basal knobs. Moreover, granular elements with characteristics similar to those of the interchromatin granules located in the nucleoplasm can be recognized in these preparations.

REFERENCES

1. Brasiello, A. R. 1968. Autoradiographic study of ribonucleic acid synthesis during spermatogenesis of *Asellus aquaticus* (crust. Isopoda). *Exp. Cell Res.* **53**:252.
2. Caro, L. G., and R. P. Van Tubergen. 1962. High resolution autoradiography. I. Methods. *J. Cell Biol.* **15**:173.
3. Darnell, J. E. 1968. Ribonucleic acids from animal cells. *Bacteriol. Rev.* **32**:262.
4. Darnell, J. E., L. Philipson, R. Wall, and M. Adesnik. 1971. Polyadenylic acid sequences: Role in conversion of nuclear RNA into messenger RNA. *Science (Wash. D. C.).* **174**:507.
5. Das, N. K., and M. Alfert. 1966. Nucleolar RNA synthesis during mitotic and meiotic prophase. *Natl. Cancer Inst. Monogr.* **23**:337.
6. Das, N. K., E. P. Siegel, and M. Alfert. 1965. Synthetic activities during spermatogenesis in the locust. *J. Cell Biol.* **25**:387.
7. Fakan, S., and W. Bernhard. 1971. Localisation of rapidly and slowly labelled nuclear RNA as

visualized by high resolution autoradiography. *Exp. Cell Res.* **67**:129.

8. GALL, J. G., and H. G. CALLAN. 1962. H^3-uridine incorporation in lampbrush chromosomes. *Proc. Natl. Acad. Sci. U. S. A.* **48**:562.
9. GRANBOULAN, N., and P. GRANBOULAN. 1965. Cytochimie ultrastructurale du nucleole. II. Etude des sites de synthese du RNA dans le nucleole et le noyau. *Exp. Cell Res.* **38**:604.
10. HENDERSON, S. A. 1963. Differential ribonucleic acid synthesis of X and autosomes during meiosis. *Nature (Lond.).* **200**:1235.
11. HENDERSON, S. A. 1964. RNA synthesis during male meiosis and spermiogenesis. *Chromosoma.* **15**:345.
12. HSU, T. C., J. E. K. COOPER, M. L. MACE, and B. R. BRINKLEY. 1971. Arrangement of centromeres in mouse cells. *Chromosoma.* **34**:73.
13. LITTAU, V. C., V. G. ALLFREY, J. H. FRENSTER, and A. E. MIRSKY. 1964. Active and inactive regions of nuclear chromatin as revealed by electron microscope autoradiography. *Proc. Natl. Acad. Sci. U. S. A.* **52**:93.
14. MONESI, V. 1965. Synthetic activities during spermatogenesis in the mouse. *Exp. Cell Res.* **39**:197.
15. MONESI, V. 1965. Differential rate of ribonucleic acid synthesis in the autosomes and sex chromosomes during male meiosis in the mouse. *Chromosoma.* **17**:11.
16. MOORE, G. P. M. 1971. DNA-dependent RNA synthesis in fixed cells during spermatogenesis in mouse. *Exp. Cell Res.* **68**:462.
17. MOSES, M. J. 1968. Synaptinemal complex. *Ann. Rev. Genet.* **2**:363.
18. MURAMATSU, M., T. UTAKOJI, and H. SUGANO. 1968. Rapidly-labelled nuclear RNA in chinese hamster testis. *Exp. Cell Res.* **53**:278.
19. NOEL, J. S., W. C. DEWEY, J. H. ABEL, and R. P. THOMPSON, 1971. Ultrastructure of the nucleolus during the Chinese hamster cell cycle. *J. Cell Biol.* **49**:830.
20. OAKBERG, E. F. 1957. A description of spermiogenesis in the mouse and its use in analysis of the cycle of the seminiferous epithelium and germ cell renewal. *Am. J. Anat.* **99**:391.
21. OAKBERG, E. F. 1957. Duration of spermatogenesis in the mouse. *Nature (Lond.)* **180**:1137.
22. OHNO, S., W. D. KAPLAN, and R. KINOSITA. 1957. Heterochromatic regions and nucleolus organizers in chromosomes of the mouse, *Mus musculus. Exp. Cell Res.* **13**:358.
23. PARCHMAN, L. G., and K. C. LIN. 1972. Nucleolar RNA synthesis during meiosis of lily microsporocytes. *Nat. New Biol.* **239**:235.
24. POLANI, P. E. 1972. Centromere localization at meiosis and the position of chiasmata in the male and female mouse. *Chromosoma.* **36**:343.
25. PRESCOTT, D. M., and M. A. BENDER. 1962. Synthesis of RNA and protein during mitosis in mammalian tissue culture cells. *Exp. Cell Res.* **26**:260.
26. SACHS, L. 1955. The possibilities of crossing-over between the sex chromosomes of the house mouse. *Genetica.* **27**:309.
27. SALPETER, M. M., and L. BACHMANN. 1972. Autoradiography. *In* Principles and Techniques of Electron Microscopy. Biological Applications. Vol. 2. M. A. Hayat, editor. Van Nostrand Reinhold Co., New York. 221–278.
28. SALPETER, M. M., and M. SZABO. 1972. Sensitivity in electron microscope radioautography using Ilford L4 emulsion: the effect of radiation dose. *J. Histochem. Cytochem.* **20**:425.
29. SCHNEDL, W. 1972. End-to-end association of X and Y chromosomes in mouse meiosis. *Nat. New Biol.* **236**:29.
30. SOLARI, A. J. 1970. The spatial relationship of the X and Y chromosomes during meiotic prophase in mouse spermatocytes. *Chromosoma.* **29**:217.
31. SOLARI, A. J., and L. L. TRES. 1967. The localization of nucleic acids and the argentaffin substance in the sex vesicle of mouse spermatocytes. *Exp. Cell Res.* **47**:86.
32. STERN, H., and Y. HOTTA. 1969. Biochemistry of meiosis. *In* Handbook of Molecular Cytology. A. Lima-de Faria, editor. American Elsevier Publishing Co., Inc., New York. **15**: 520–539.
33. TAYLOR, J. H. 1960. Nucleic acid synthesis in relation to the cell division cycle. *Ann. N. Y. Acad. Sci.* **90**:409.
34. TRES, L. L., A. L. KIERSZENBAUM, and C. J. TANDLER. 1972. Inorganic cations in cell nucleus. Selective accumulation during meiotic prophase in mouse testis. *J. Cell Biol.* **53**:483.
35. UTAKOJI, T. 1966. Chronology of nucleic acid synthesis in meiosis of the male Chinese hamster. *Exp. Cell Res.* **42**:585.
36. WISSE, E., and A. D. TATES. 1968. A gold latensification Elon ascorbic acid developer for Ilford L4 emulsion. *Proc. 4th Eur. Reg. Conf. Electron Microscopy, Rome.* 465.
37. WOLLAM, D. H. M., and E. H. R. FORD. 1964. The fine structure of the mammalian chromosome in meiotic prophase with special reference to the synaptinemal complex. *J. Anat.* **98**:163.
38. YASMINEH, W. G., and J. J. YUNIS. 1970. Localization of mouse satellite DNA in constitutive heterochromatin. *Exp. Cell Res.* **59**:69.